International Journal of Research (IJR)

p-ISSN: 2348-6848
e-ISSN: 2348-795X
Vol. 9 Issue 01
January 2022

PR And fuzzy Logic control Control Three-phase of Bi-directional Z-source Converters a Low-harmonic for Vehicle-to-Grid Applications

M.ROHIT[1], CH.RAJA SRI [2], M.RAVINDER [3]

[1] Asst, prof ,Dept, of Electrical and Electronics Engineering , Holy Mary Institute of Technology and Science, Hyderabad, Telangana, India. Email id: muderohit@gmail.com.
[2] Asst, prof ,Dept, of Electrical and Electronics Engineering , Holy Mary Institute of Technology and Science, Hyderabad, Telangana, India. Email id: :rajasri045@gmail.com.
[3] Asst, prof ,Dept, of Electrical and Electronics Engineering , Holy Mary Institute of Technology and Science, Hyderabad, Telangana, India. Email id:ravinder.m@hmgi.ac.in

Abstract— *Three-phase Z-source inverters provide a solution of voltage boosting by a single-stage topology. They are also capable of bi-directional operation as rectifiers, thus have great potential for applications in the field of transportation electrification such as Vehicle-to-Grid (V2G) chargers. In this paper, three new modulation schemes for three-phase Z-source converters are proposed and investigated. The best performed one is further developed to a closed-loop PR And fuzzy control method. While the voltage conversion ratio is flexible, the output voltage Total Harmonics Distortion (THD) is below 3% within the voltage ratio range of 0.5 to 2.5. The effectiveness of the proposed method has been fully validated in MATLAB/Simulink simulations Compared to existing control methods, the proposed one performs better with reduced harmonics, flexible voltage gain, and simpler control algorithm.*

Index Terms—Z-source converter, Bi-directional converter, shoot-through states, voltage harmonics, closed-loop closed- loop PR And fuzzy control method.

I. INTRODUCTION

There is an increasing demand for advanced power converters and their corresponding control algorithms in the field of transportation electrification in general, and railway electrification in specific [1]. Traditional full-bridge three phase inverter is a fundamental topology for energy transformation between Direct Current (DC) voltage sources such as vehicle batteries and three-phase Alternating Current (AC) power grids, microgrids or loads. However, in the control and operation of traditional full-bridge inverters, dead time between the two switches in the same bridge is required to avoid short-circuit failures [2].

The existence of dead time unavoidably brings AC output waveform distortions. Moreover, when there is a large difference in voltage level between the output AC side and the input DC side, one more DC-DC converter is often added in the inverter to regulate output voltage level. This two-stage system configuration not only decreases the efficiency but also weakens the dynamic response of the system with regard to both disturbances in environmental conditions and grid perturbations [3].

A Z-source inverter [4] and a quasi-Z-source inverter [5] were proposed to overcome the above barriers of traditional two-stage voltage-source inverters. As shown in Fig. 1, shape impedance network composed of two inductors LZ1, LZ2 and two capacitors CZ1, CZ2 is combined in a traditional three phase full-bridge inverter [6]. Because of the existence of the X-shape impedance network, it is possible to turn on the two none bridge simultaneously without short-circuited the Input voltage source [4]. Moreover, the Z-source inverters take advantage of the shoot-through states ingeniously to achieve voltage boosting without any additional switches or control circuitry [7].

Therefore, the Z-source inverters could achieve voltage buck and boosting by a single-stage topology with high robust. The voltage level of different microgrids could vary considerably, which makes the Z-source converters more advantageous in the process of EV batteries' feeding to
the grids. The Z-source inverter could also operate bidirectionally, which is essential in V2G applications. The input diode Dr is connected in parallel with a switch S1. When switch S1 is turned on, the Z-source inverter could operate as a conventional three-phase PWM rectifier.

Because of the above-mentioned features, Z-source converters have been widely investigated in areas of not only EV charging [8] [9], but also EV motor drive [10] [11], PV solar energy system [12] [13], wireless energy transfer [14] [15] and integration of microgrid [16] [17]. The increasing voltage gain capability and modulation indexes of both rectifier and inverter stages are advantages of three-phase Z-source converters [18]. Different approaches of applying bi-directional Z-source inverters in V2G applications have been investigated [19] [20].

Paper [21] provided an overall introduction and comparison of space vector modulation schemes for three-phase Z-source inverters. Besides the basic Z-source impedance topology, many modified Z-source topologies have been developed [22]- [24] to reduce switching loss and improve power density. Though these proposed converters based on Z-source topology could generally achieve smaller size and wider voltage conversion ratio, they have issues in complicated structure, instability, voltage stress of switches, power level limitation [24] and output harmonics [7] [25].

Therefore, this paper aims to improve the performance of converter by designing and optimizing the control method of a basic three-phase Z-source converter, rather than adding more devices or complicated circuits. India has relatively long sunny days for more than ten months and partly cloudy sky for most of the days i.e. almost two months. This makes India very rich in solar energy especially desert sides in west which include Gujarat, Rajasthan, Madhya Pradesh etc. Photovoltaic Panel or modules are used directly to create electricity.

Besides this solar panels however, it also needs "Balance of System" components including inverters, wiring, breakers and switches, which can account for up to half of the system cost. Inverters like string inverters, micro-inverters are used with PV panels. In string inverters the several numbers of panels are connected in series with one centralized inverter, while micro-inverter invert the electricity from single PV panel, as each panel has a single inverter attached beyond it.

Micro-inverter is an upcoming field of research in PV technology as it has more advantage

p-ISSN: 2348-6848
e-ISSN: 2348-795X
Vol. 9 Issue 01
January 2022

over other PV systems. It is used as plug and play devices. Typically, the micro inverter are design for lower ranges; as the capacity of solar panel increases, the size of micro-inverter should increases as well[1,2]. In this paper the simulation of micro-inverter is discussed with analysis of control techniques of it

Because of the above-mentioned features, Z-source converters have been widely investigated in areas of not only EV charging [8] [9], but also EV motor drive [10] [11], PV solar energy system [12] [13], wireless energy transfer [14] [15] and integration of microgrid [16] [17]. The increasing voltage gain capability and modulation indexes of both rectifier and inverter stages are advantages of three-phase Z-source converters [18]. Different approaches of applying bi-directional Z-source inverters in V2G applications have been investigated [19] [20]. Paper [21] provided an overall introduction and comparison of space vector modulation schemes for three-phase Z-source inverters.

Besides the basic Z-source impedance topology, many modified Z-source topologies have been developed [22]-[24] to reduce switching loss and improve power density. Though these proposed converters based on Z-source topology could generally achieve smaller size and wider voltage conversion ratio, they have issues in complicated structure, instability, voltage stress of switches, power level limitation [24] and output harmonics [7] [25]. Therefore, this paper aims to improve the performance of converter by designing and optimizing the control method of a basic three-phase Z-source converter, rather than adding more devices or complicated circuits.

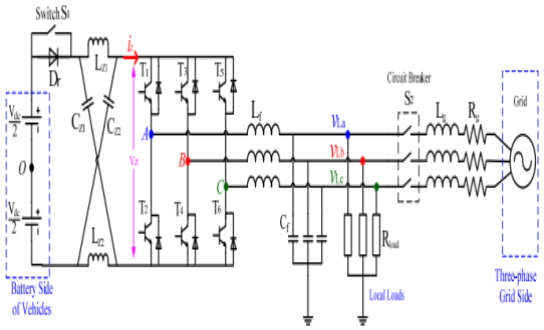

Fig.1 Topology of a bi-directional three-phase Z-source converter

Some advanced control logic for three-phase Z-source converters has been proposed to achieve better dynamic performance [26]-[28], realize ZVS rectifying [29], reduce grid current distortion [30], decouple active and reactive power [3] and increase voltage conversion ratio [31]. However, these control methods require tremendous and complicated calculations to meet the special requirements of designated applications with more passive devices added. Those control schemes are often complicated [32].

In this paper, three new modulation schemes of inserting shoot-through states are proposed. Among them, sine variable modulation shows better performance over harmonic suppression and is therefore further developed into a closed loop control method.

The converter could be connected to the grid or a three-phase load. The switch S1 and circuit breaker S2 determine the working mode. To simplify the calculation, the input DC voltage source is divided into two voltage sources, each has the magnitude of ***Vdc***/2, and the middle point is labeled as ***O***. Compared to conventional control schemes, the proposed method in this paper has the following advantages: low harmonics in output voltage and current; support of bidirectional operation; easy to implement without complicated algorithm or computation burden; easy to modify for the control in grid-connected mode

II. PROPOSAL OF CONTROL METHODS AND ANALYSIS

A. Basic Principle of Three-phase Z-source inverters

Fig. 1 shows the three-phase Z-source inverter which consists of a Z-source topology, a diode D_r and a traditional three-phase full-bridge inverter. The Z-source topology is composed of two inductors L_{Z1}, L_{Z2} and two capacitors C_{Z1}, C_{Z2}.To achieve the symmetrical characteristic, the two inductors usually would have the same inductance, i.e. $L_{Z1}=L_{Z2}=\boldsymbol{Lz}$, while

The two capacitors also would have the same capacitance, i.e. $C_{Z1}=C_{Z2}=\boldsymbol{Cz}$. Otherwise, an asymmetric topology would lead to unbalanced operation as well as difference in voltage and current stress of devices [33]. The output side of the Z-source topology is connected to a classical three-phase full-bridge inverter with six switches. The diode D_r is placed in series with the DC voltage source to block any reverse current from the Z source topology in order to achieve voltage boosting [33].

When circuit breaker S_1 is turned on, the converter operates bi-directionally as a rectifier and power transfers from the grid to the DC side of the converter. The Z-source network acts as a special LC filter of the three-phase rectifier. Traditional SPWM control method of three-phase full bridge rectifiers is applicable. When circuit breaker S_1 is turned off, the converter operates as an inverter and power transfers from the DC side to the thre phase loads or the grid. Circuit breaker S_2 determines whether the converter operates in grid-connected mode or resistive load mode.

The voltage-boosting principle of three-phase Z-source inverters is similar to the one of single-phase ones as described in [33], and therefore the detailed analysis and equivalent circuits in each state are not repeated here. In short, the voltage $\boldsymbol{Vz}$ is boosted higher than the input voltage $\boldsymbol{V_{dc}}$ because of shoot through states. In steady state, the operation of Z-source inverter is divided into two periods: shoot-through states and non-shoot-through states [33]. It is assumed that the total time of shoot-through states in one switching cycle is $\boldsymbol{T_s}$, and the period of one cycle is $\boldsymbol{T}$, then the shoot-through duty ratio $\boldsymbol{D}$ of shoot-through states is

$$D = \frac{T_1}{T} \tag{1}$$

Equation (2) shows the state space equation:

$$\frac{d}{dt}\begin{bmatrix} i_{LZ1}(t) \\ i_{LZ2}(t) \\ v_{CZ1}(t) \\ v_{CZ2}(t) \end{bmatrix} = \begin{bmatrix} 0 & 0 & \frac{2D-1}{L_z} & 0 \\ 0 & 0 & 0 & \frac{2D-1}{L_z} \\ \frac{-D}{C_z} & \frac{1-D}{C_z} & 0 & 0 \\ \frac{1-D}{C_z} & \frac{-D}{C_z} & 0 & 0 \end{bmatrix} \cdot \begin{bmatrix} i_{LZ1}(t) \\ i_{LZ2}(t) \\ v_{CZ1}(t) \\ v_{CZ2}(t) \end{bmatrix} + \begin{bmatrix} \frac{1-D}{L_z} \\ \frac{1-D}{L_z} \\ 0 \\ 0 \end{bmatrix} \cdot V_{dc} + \begin{bmatrix} 0 \\ 0 \\ \frac{D-1}{C_z} \\ \frac{D-1}{C_z} \end{bmatrix} \cdot i_z \tag{2}$$

The steady-state parameters could be obtained by setting (2) to zero, as shown in (3):

$$\begin{cases} \overline{i_{LZ_1}} = \overline{i_{LZ_2}} = \frac{1-D}{1-2D} \cdot \overline{i_Z} \\ \overline{v_{CZ_1}} = \overline{v_{CZ_2}} = \frac{1-D}{1-2D} \cdot V_{dc} = \overline{V_Z} \\ v_{Z-peak} = \frac{1}{1-2D} \cdot V_{dc} \end{cases} \tag{3}$$

Since $\boldsymbol{D}$ must be greater than 0 and smaller than 1, the average magnitude of the output voltage across the Z-source topology $\boldsymbol{Vz}$ is boosted higher than input DC voltage $\boldsymbol{V_{dc}}$ as shown in (3). When more shoot-through states are inserted, the output voltage gain will become higher [34]. The voltage gain of Z-source inverters could be infinite theoretically, whereas the effect of parasitic components and harmonics requirement limits the maximum practical gain.

The core concept of Z-source converter's control is to boost voltage by inserting shoot-through states while reducing output harmonics and power loss [33]. Three shoot-through states inserting methods are proposed below for three-phase Z-source converters.

B. Proposed Modulation Schemes

A study of inverters connected to resistive loads is presented here. Single-phase-leg modulation schemes [35]. Each subcategory could be further divided by continuous modulation methods and discontinuous closed-loop PR and fuzzy control method. Control methods of three-phase Z-source inverters could be classified into two categories: shoot-through of three-phase leg modulation schemes and shoot-through of modulation methods. If only

International Journal of Research (IJR)
p-ISSN: 2348-6848
e-ISSN: 2348-795X
Vol. 9 Issue 01
January 2022

one bridge is inserted with shoot through states, then the high current during shoot-through states would all flow into the two switches of this bridge. Switches of the other two bridges do not share the same current stress, which leads to the asymmetry of the topology and the operation.

Therefore, the three-phase-leg modulation scheme is selected for the proposed methods. In non-shoot-through states, its operation is divided by zero states and non-zero states [35]. Based on this, there are three primary subcategories of inserting shoot-through states: (1) Simple boost control: part of zero states are converted into shoot-through states; (2) Maximum boost control: all zero states areas are converted into shoot-through states; (3) Constant boost control: most of zero states areas are converted into shoot through states [35] [36]. The proposed methods of inserting shoot-through states are based on conventional SPWM scheme of three-phase full-bridge inverters and belong to constant boost control.

Three sinusoidal modulating signals at the frequency of the desired output but displaced from each other by 2π/3 phase are generated. The triangular carrier wave is compared with the modulation waves to generate six gate signals. The concept is modifying the magnitude of three modulation waves to create overlaps. In Fig. 2(a), the sine modulation waves of generating signals for switch T_1 and T_2 in phase A bridge are presented.
The black solid curve represents a standard sine wave whose magnitude ranges from $-M$ to M, where $0 < M < 1$.

Two more modulation waveforms are derived by adding a variable ***b(t)*** which varies with time respectively. The red dashed modulation wave is used for generating gate signals for upper switch T_1, which is marked as w_{T1}. The blue dotted modulation wave is used for generating gate signals for lower switch T_2, which is marked as w_{T2}. Fig. 2(b) is a zoomed view of the circled part of Fig. 2(a). It shows the overlap of switching signals G_{T1} and G_{T2} by two different modulation waves. For simplicity, ***b(t)*** is set as a constant in Fig. 2

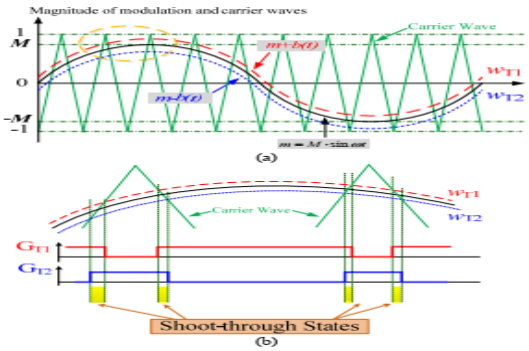

Fig.2 Shoot-through states inserting by overlap: (a) Modulation waves in one cycle; (b) Zoomed view

$$\begin{cases} m_A = M \cdot \sin \omega t \\ m_B = M \cdot \sin(\omega t - \frac{2}{3}\pi) \\ m_C = M \cdot \sin(\omega t - \frac{4}{3}\pi) \end{cases} \quad (4)$$

The magnitudes of three modulation waves for each bridge are shown in (4), where ***M*** represents the magnitude of sine modulation waves; and m_A, m_B and m_C represent the instantaneous magnitude of modulation waves of phase A, B and C. Both m_A, m_B and m_C range from $-M$ to M. The three modulation waves are compared to the carrier waves in Fig. 2(b), then six pulsed gate signals are generated accordingly as shown in Fig. 3.

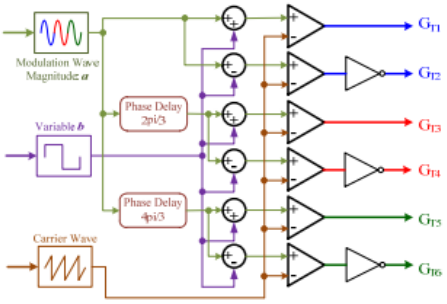

Fig.3 Generation of switching signals to insert shoot-through states

For the cosine variable modulation, ***b(t)*** is a cosine function which has the same phase with the corresponding modulation waves as presented in equation (7) and Fig. 5(b). In other words, ***b(t)*** could be regarded as a sine function which has a π/2 phase delay with the modulation wave. The shoot-through states are inserted more in valleys of the modulation wave, and are inserted less in the peaks of modulation waves.

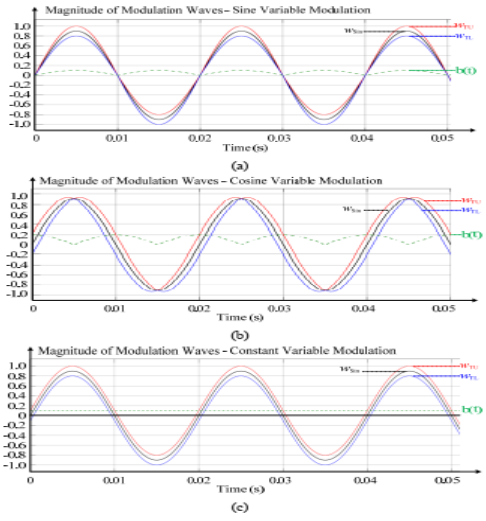

Fig.5 Modulation waves and corresponding magnitudes of *b(t)*: (a) Sine variable modulation; (b) Cosine variable modulation; (c) Constant variable modulation

For the constant variable modulation, the absolute value of ***b (t)*** is equal to a constant. The constant value is defined as $2B/\pi$ as shown in (8), which is the same with the average magnitude of sine variable modulation as well as cosine variable modulation during one cycle. Thus, it is easy to analyze and compare the three proposed modulation schemes.

$$\begin{cases} b_1(t)=B\cdot\dfrac{[\cos(\omega t)+1]}{2} & b_2(t)=B\cdot\dfrac{-[\cos(\omega t)+1]}{2} \\ b_3(t)=B\cdot\dfrac{\left[\cos(\omega t-\frac{2}{3}\pi)+1\right]}{2} & b_4(t)=B\cdot\dfrac{-\left[\cos(\omega t-\frac{2}{3}\pi)+1\right]}{2} \\ b_5(t)=B\cdot\dfrac{\left[\cos(\omega t-\frac{4}{3}\pi)+1\right]}{2} & b_6(t)=B\cdot\dfrac{-\left[\cos(\omega t-\frac{4}{3}\pi)+1\right]}{2} \end{cases} \quad (7)$$

For the constant variable modulation, the absolute value of ***b(t)*** is equal to a constant. The constant value is defined as $2B/\pi$ as shown in (8), which is the same with the average magnitude of sine variable modulation as well as cosine variable modulation during one cycle. Thus, it is easy to analyze and compare the three proposed modulation schemes.

$$\begin{cases} b_1(t)=b_3(t)=b_5(t)=\dfrac{2}{\pi}B \\ b_2(t)=b_4(t)=b_6(t)=-\dfrac{2}{\pi}B \end{cases} \quad (8)$$

C. Voltage Gain Analysis

As described before, the input voltage V_{dc} is boosted to V_Z by the Z-source topology with the insertion of shoot-through states, then the AC output voltage is higher than the input DC voltage source. The Z-source topology could be regarded as a front-end boost converter for a DC-AC inverter. Bridge voltages V_{AO}, V_{BO} and V_{CO} would vary among $+/2\,V_Z$, 0, $-/2\,V_Z$. According to (3), the peak value of phase voltages could be obtained as:

$$\hat{V}_{AO}=\hat{V}_{BO}=\hat{V}_{CO}=\frac{\hat{V}_m}{\hat{V}_{ca}}\cdot\frac{\bar{V}_Z}{2}=M\cdot\frac{\bar{V}_Z}{2}=\frac{M\cdot(1-D)}{1-2D}\cdot\frac{V_{dc}}{2} \quad (9)$$

where $\hat{V}_m$ represents the maximum and peak value of the sine wave. $\hat{V}_{ca}$ represents the peak magnitude of the carrier wave. The modulation ratio is defined as ***M***, which represents $V\,V$. It is obvious that the shoot-through duty ratio ***D*** in the three proposed modulation schemes is directly determined by ***M*** and ***B***. Because the frequency of the modulation wave is much smaller than that of the carrier wave, the magnitude of modulation wave could be assumed as constant during one switching cycle.

Fig. 6 shows the modulation waveforms within a very short time. In Fig. 6, the black line w_{sin} represents the standard sine waveform, the red line w_{TU} represents the modified modulation wave to generate gate signals for the upper switch, and the blue curve w_{TL} represents the modified modulation wave to generate gate signals for the lower switch in the bridge. The green curve ***WC*** represents the carrier wave during this short period; it is assumed that the magnitudes of each modulation wave are constant. There is another assumption that the switching frequency of carrier wave is high enough to calculate the ideal duty cycle ***D***. In Fig. 6, the total time length of shoot-through states in one period of the carrier wave is $2t$.

The duty ratio of one bridge D_B is equal to $2t/T$. Since there are three bridges in the full-bridge inverter, the total duty ratio ***D*** is equal to $3D_B$. The time slots when shoot-through states are inserted in two or three bridges simultaneously would occur when the instant magnitudes of modulation waves of two bridges are equal or very close to each other. These time slots normally account for very little portion and are thus neglected unless ***B*** is very large. The following equations could be obtained:

$$\frac{r}{t}=\frac{2R}{T} \quad (10)$$

International Journal of Research (IJR)
p-ISSN: 2348-6848
e-ISSN: 2348-795X
Vol. 9 Issue 01
January 2022

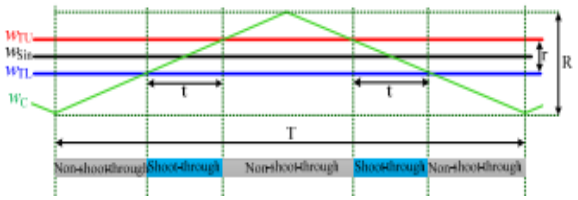

In Fig. 7, the relationship between ideal overall voltage gain *G* and parameter *B* is presented. The overall voltage gain increases with the increase of modulation index *M* and parameter *B*.

SIMULATION RESULTS

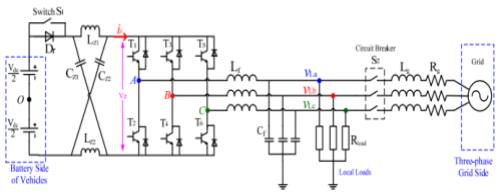

Fig.1 Topology of a bi-directional three-phase Z-source converter

Open-loop simulations have been conducted in Matlab Simulink. The DC side voltage ***Vdc*** is set as 500V to represent a typical EV battery voltage. The balanced three-phase loads are composed of three resistors whose resistance Rload is 112.5Ω in star connection, LZ1=LZ2=280μH, CZ1=CZ2=141μF, Lf=8.95mH Cf=7μF, AC output frequency f=50Hz. The calculation of these parameters is presented in the Appendix.

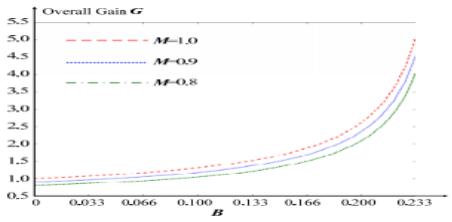

Fig.7 Relationship between the overall gain *G* and parameter *B First,*

the simulation at rated output voltage of sine variable method is conducted. The peak magnitude of rated output phase voltage is set as 1060V, whose r.m.s. value is 750V at the medium voltage level. Fig. 8 shows the waveforms of three output phase voltages ***VLA***, ***v***Lb and ***v***Lc respectively. The THD of each phase voltage is only 2.66%.

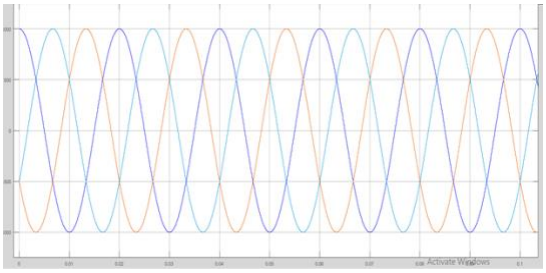

Fig. 8 Output phase voltages of sine variable method at rated output voltage

To further investigate the difference among the three methods on output voltage harmonics, open-loop simulations have been conducted with ***M***=0.9 and ***B***=0.25 such that the magnitude of modified modulation waves would go beyond the magnitude of the carrier wave and the output harmonics would increase undoubtedly.

In this way, the effect of the three control methods on output harmonics could be clearly illustrated. Waveforms of output phase voltages are presented in Fig. 9. It is clear that with such a large value of ***B***, the output harmonic of sine variable method still maintains within a low level. In contrast, the harmonics of cosine variable method is much greater. The harmonics level of constant variable method is slightly lower than one of cosine variable method, but the voltage magnitude is lower than expected.

This is because the total duration of the shoot-through states in a three-phase topology has become too long, and the average magnitude of both the capacitor voltage *VCZ1*, *VCZ2* and voltage ***VZ*** could not reach the ideal values in (3). The harmonic analysis plots of three methods are shown in Fig. 10. The cosine variable method produces the highest 5^{th} order harmonics. The 5th, 7th and 11th order

p-ISSN: 2348-6848
e-ISSN: 2348-795X
Vol. 9 Issue 01
January 2022

harmonics account for most of the total harmonics in the three methods, while there is little even order harmonics because of the symmetricity of the control logic.

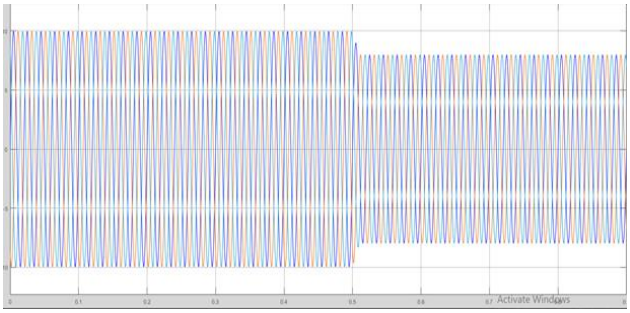

Fig. 11(a) represents the relationship between the THD of phase voltage *VLA* and parameter *B* when *M*=0.9.

As the magnitude and frequency of output phase voltage ***VLa*** are the same as ***VLb*** and ***VLc***, only ***VLa*** is presented as a representative.

The THD increases as ***B*** increases because of the shoot-through states insertion. Cosine variable method has the greatest output harmonics, while sine variable method leads to lowest output harmonics. For sine variable method, the total THD of output phase voltage ***VLa*** is only 2.83% when ***B***=0.2, which means the magnitude of the modified modulation wave already exceeds the magnitude of the carrier wave. Since the output load is resistive, the voltage distortion and current distortion are the same. For reference, the harmonics of 2nd – 19th orders are compared with the limits in Fig. 10(d). It is clear that the output harmonics are well below harmonic limits

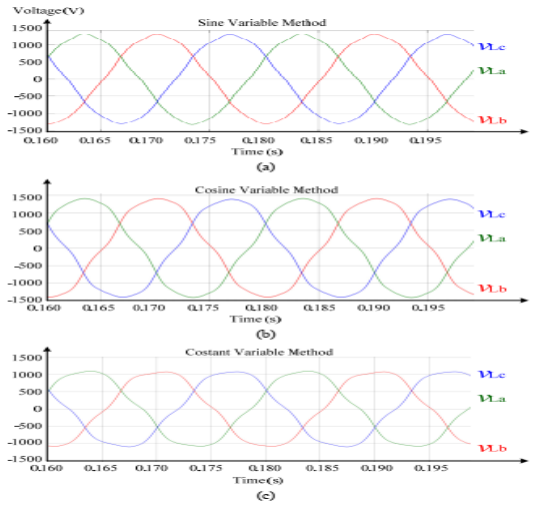

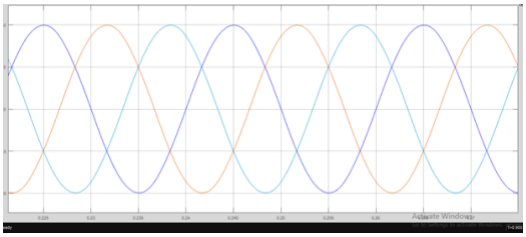

Fig. 9 Waveforms of output phase voltages with high shoot-through duty ratio *D*: (a) Sine variable method; (b) Cosine variable method; (c) Constant variable method

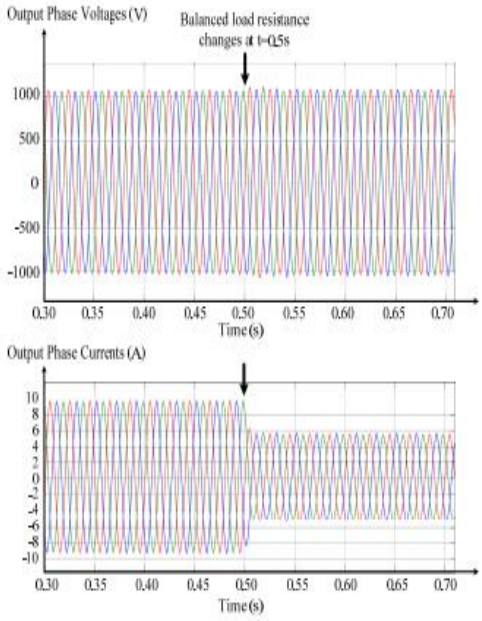

International Journal of Research (IJR)
p-ISSN: 2348-6848
e-ISSN: 2348-795X
Vol. 9 Issue 01
January 2022

Fig.14 Simulation waveforms of output phase voltages and currents when R load changes

Proportional Resonant Controller

In proportional controller the output is proportional to the error signal. The proportional resonant controller is one of the most popular controllers used to regulate the injected current into the grid. The PR controller can overcome few drawbacks of the proportional integral controller. A PR controller is a combination of a proportional term and a resonant term which can be expressed mathematically as PR controller is designed to achieve 0.1% maximum steady-state error at 50Hz frequency. The designed PR controller (*TPR(s)*) is given by:

$$T_{PR}(s) = \frac{s^2 + 314.1s + 98596}{s^2 + 0.314s + 98596}$$

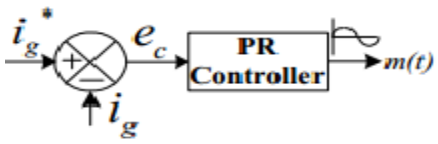

Fig. 6. The current control strategy for the [25]

In order to improve the performance by handling harmonics a harmonic compensator is incorporated. this harmonic compensator can be expressed as:

$$C_{RC}(s) = \sum_{K=3,5,7\ldots} K_{ih} \frac{s}{s^2 + (\omega h)^2} \quad (10)$$

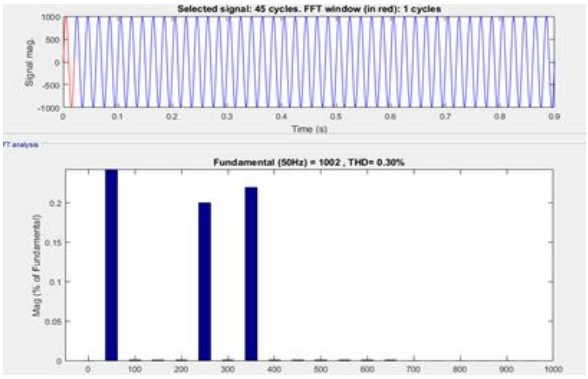

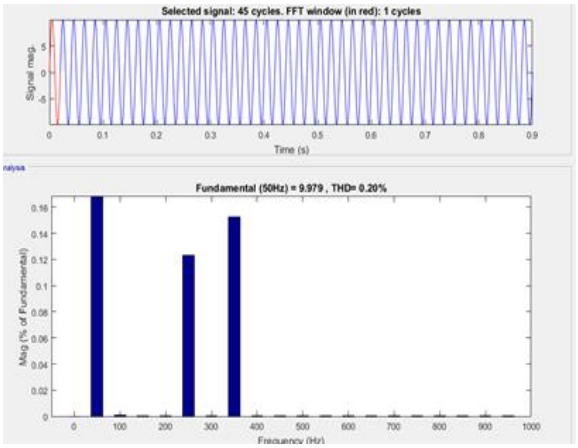

THD PR control fuzzy Logic control

e_V	Δe_V				
	AV	PS	PB	NS	NB
AV	AV	PS	PB	NS	NB
PS	PS	PB	PB	AV	NS
PB	PB	PB	PB	PS	AV
NS	NS	AV	PS	AV	NS
NB	NB	NS	AV	NB	NB

Figure 7: FLC in three stages

Method of de fuzzification with centroid

In figure 10, presented polyhedron map which represents the fuzzy output rules by using MM (Minimum of maximum) method.

Rule1: Calculation of minimum membership value or grade It can be calculated form minimum value that extracts fromintersections of variables of input say x1, x2 and maximum is taken by rescaling output rule.

Rule2: Calculation of fuzzy output

It can be calculated by using centroid in defuzzificationstage [10] represents as,

$$K_f = \frac{\int y\, \mu(y)\, dy}{\int \mu(y)\, dy}$$

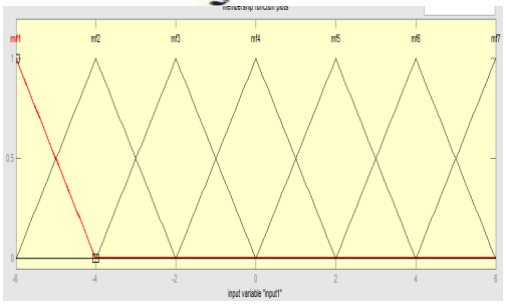

8(a): Voltage error Membership function

International Journal of Research (IJR)
p-ISSN: 2348-6848
e-ISSN: 2348-795X
Vol. 9 Issue 01
January 2022

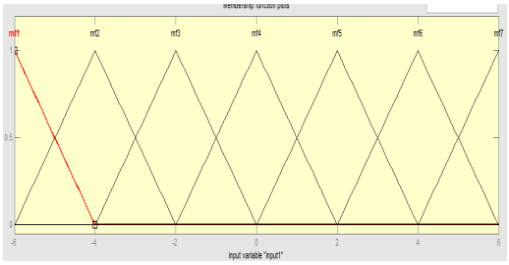

8(b): Rate of change in voltage error membership function

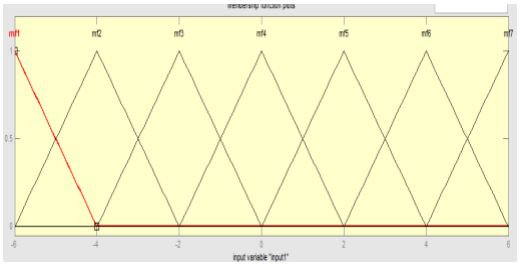

8(c): Variable K_{IV} Membership function

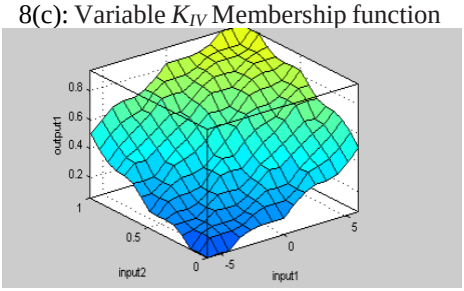

8(d): Fuzzy surface Figure

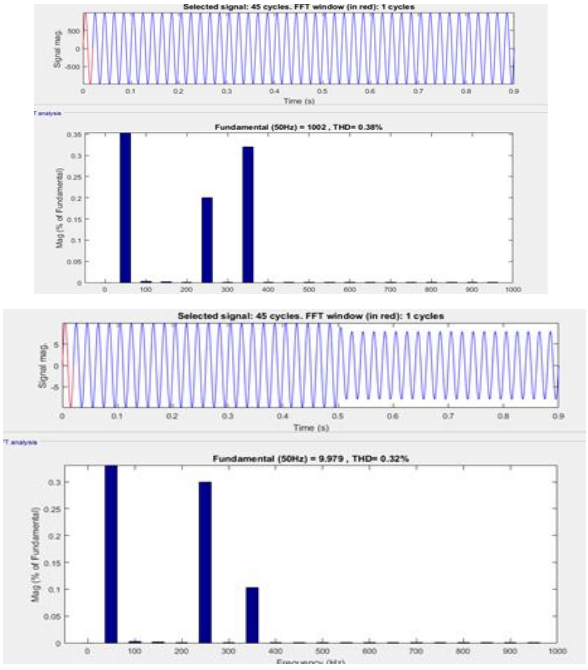

THD fuzzy Logic

VI. CONCLUSIO

The theoretical analysis, simulation and results in the paper proved the good performance of the proposed methods for bi-directional three-phase Z-source converters. Shoot-through states are inserted sinusoidally, and the output three-phase voltages could be boosted while the harmonics are maintained within a low level. Constant variable method, sine variable method and cosine variable method are introduced and compared. Sine variable method produces least harmonics, and is further developed PR And fuzzy control method. Control methods of three-phase Z-source inverters could be classified into two categories: shoot-through of three-phase leg modulation schemes and shoot-through of modulation methods. Steady-state waveforms in experiment results proved the capability of voltage boosting with all circuitry waveforms matched the theoretical analysis. Transient waveforms showed the dynamic response with the disturbance of input voltage and load resistance.

The output phase voltages could catch the reference quickly and smoothly. Compared to existing control methods, the proposed one has better performance on harmonics suppression with an uncomplicated control algorithm, thus would be suitable for its application in vehicle chargers with bi-directional power flow between the vehicle batteries and the three-phase AC bus of a microgrid.

The future work mainly includes the implementation of an EV charger prototype to testify the charging performance and conversion efficiency in a Power suppression of the input current spikes and the advanced control in unbalanced load cases.

REFERENCES

[1] S. A. Singh, G. Carli, N. A. Azeez and S. S. Williamson, "A modified Z source converter based single phase PV/grid inter-connected DC charging

converter for future transportation electrification," *2016 IEEE Energy Conversion Congress and Exposition (ECCE)*, Milwaukee, WI, 2016, pp. 1-6.
[2] Yushan Liu, Haitham Abu-rub, Gaoming Ge, "Z-Source Quasi Z Source Inverters Derived Networkds Modulations", *IEEE Industrial Electronics Magazine*, Dec 2014
[3] S. Jain, M. B. Shadmand and R. S. Balog, "Decoupled Active and Reactive Power Predictive Control for PV Applications Using a Grid-Tied Quasi-Z-Source Inverter," *IEEE Journal of Emerging and Selected Topics in Power Electronics*, vol. 6, no. 4, pp. 1769-1782, Dec. 2018.
[4] Fang Zheng Peng, "Z-source inverter," *IEEE Transactions on Industry Applications*, vol. 39, no. 2, pp. 504-510, March-April 2003.
[5] Miaosen Shen, Jin Wang, A. Joseph, Fang Zheng Peng, L. M. Tolbert and D. J. Adams, "Constant boost control of the Z-source inverter to minimize current ripple and voltage stress,"
[6] Y. Liu, H. Abu-Rub, Y. Xue and F. Tao, "A Discrete-Time Average Model-Based Predictive Control for a Quasi-Z-Source Inverter," *IEEE Transactions on Industrial Electronics*, vol. 65, no. 8, pp. 6044-6054, Aug. 2018.
[7] Q. Zhang, T. Na, L. Song and S. Dong, "A Novel Modulation for Soft Switching Three-Phase Quasi-Z-Source Rectifier Without Auxiliary Circuit," *IEEE Transactions on Industrial Electronics*, vol. 65, no. 6, pp. 5157-5166, Jun. 2018.
[8] Guo Feng, Fu Lixing, Lin, Chien Hui, Li Cong, Choi Woongchul, Wang Jin, "Development of an 85-kW Bidirectional Quasi-Z-Source Inverter With DC Link Feed-Forward Compensation for Electric Vehicle Applications", *IEEE Transactions on Power Electronics*, vol. 28, no. 12, pp. 5477-5488. Dec 2013
[9] Tuopu Na, Qianfan Zhang, Jiaqi Tang, and Jinxin Wang, "Active Power Filter for Single-Phase Quasi-Z-Source Integrated On-Board Charger", *CPSS Transactions on Power Electronics and Applications*, vol. 3, no. 3, Sep 2018
[10] Alexandre Battiston, El-Hadj Miliani, Serge Pierfederici, and Farid Meibody-Tabar, "Efficiency Improvement of a Quasi-Z-Source Inverter Fed Permanent-Magnet Synchronous Machine-Based Electric Vehicle," *IEEE Transactions on Transportation Electrification*, vol. 2, no. 1, pp. 14-23, 2016.
[11] Jérémy Cuenot, Sami Zaim, Babak Nahid-Mobarakeh, et al, "Overall Size Optimization of a High-Speed Starter Using a Quasi-Z-Source Inverter," *IEEE Transactions on Transportation Electrification*, vol. 3, no. 4, pp. 891-900, Dec 2017.
[12] Y. Li, S. Jiang, J. G. Cintron-Rivera and F. Z. Peng, "Modeling and Control of Quasi-Z-Source Inverter for Distributed Generation Applications," *IEEE Transactions on Industrial Electronics*, vol. 60, no. 4, pp. 1532-1541, April 2013.
[13] W. Liang, Y. Liu, B. Ge, H. Abu-Rub, R. S. Balog and Y. Xue, "Double Line-Frequency Ripple Model, Analysis, and Impedance Design for Energy-Stored Single-Phase Quasi-Z-Source Photovoltaic System.

About Authors

M. ROHIT received the B.Tech degree in Electrical & Electronics Engineering from JB institute of technology Hyderabad, Telangana India in the year 2015 & M.Tech from Geethanjali college of engineering and technology JNTU Hyderabad, Telangana, India in the year 2018.I have teaching experience of 1 years in engineering Colleges Iam currently Working as Assistant professor in Holy Mary institute of Technology & Science, Bogaram (V), Medchal District, Hyderabad, India in the Dept. of Electrical & Electronics Engineering. My area of interest in power Systems, Power Electronics& Drives HVE, FACTS RES AI, power quality.

CH.RAJASRI received the B.Tech degree in Electrical & Electronics Engineering from Gokaraju Rangaraju institute of engineering and Technology Hyderabad, Telangana India in the year 2016 & M.Tech from Vignana bharathi institute of engineering Hyderabad, A.P, India in the year 2019.I have teaching experience of 1 years in engineering Colleges Iam currently Working as Assistant professor in Holy Mary institute of Technology & Science, Bogaram (V), Medchal District, Hyderabad, India in the Dept. of Electrical & Electronics Engineering. My area of interest in power Electronics, Power Electronics& Drives HVE, FACTS RES, power quality.

p-ISSN: 2348-6848
e-ISSN: 2348-795X
Vol. 9 Issue 01
January 2022

RAVINDER.M

Completed B.Tech. in Electrical & Electronics Engineering in the year 2007 from JNTU, Hyderabad, Telangana, India and M.Tech in Electrical Power System(EPS) in the year 2017 from JNTUH, Hyderabad, Telangana, India. I have teaching experience of 7 years in Various engineering Colleges Iam currently Working as Assistant professor in Holy Mary institute of Technology & Science, Bogaram (V), Medchal District, Hyderabad, India in the Dept. of Electrical & Electronics Engineering. My area of interest in power Electronics, Power Electronics& Drives HVE, FACTS RES, power quality Power System, Power Electronics, power quality, renewable energy Resource, Hvdc FACTS